Neutronic and Photonic Analysis of UWMAK-III Blanket and Shield in Noncircular Toroidal Geometry

Y. Gohar, C.W. Maynard, and E.T. Cheng

October 1976

UWFDM-183

FUSION TECHNOLOGY INSTITUTE

UNIVERSITY OF WISCONSIN

MADISON WISCONSIN

Neutronic and Photonic Analysis of UWMAK-III Blanket and Shield in Noncircular Toroidal Geometry

Y. Gohar, C.W. Maynard, and E.T. Cheng

Fusion Technology Institute
University of Wisconsin
1500 Engineering Drive
Madison, WI 53706

http://fti.neep.wisc.edu

October 1976

UWFDM-183

"LEGAL NOTICE"

"This work was prepared by the University of Wisconsin as an account of work sponsored by the Electric Power Research Institute, Inc. ("EPRI"). Neither EPRI, members of EPRI, the University of Wisconsin, nor any person acting on behalf of either:

"a. Makes any warranty or representation, express or implied, with respect to the accuracy, completeness, or usefulness of the information contained in this report, or that the use of any information, apparatus, method, or process disclosed in this report may not infringe privately owned rights; or

"b. Assumes any liabilities with respect to the use of, or for damages resulting from the use of, any information, apparatus, method or process disclosed in this report."

UWFDM-183

Neutronic and Photonic Analysis of UWMAK-III Blanket and Shield in Non-Circular Toroidal Geometry

Y. Gohar
C. W. Maynard
E. T. Cheng

September 1976

Published in the Proceedings of the 2nd ANS Topical Meeting on the **Technology of Controlled Nuclear Fusion, held in Richland, Washington,** September 21-23, 1976.

NEUTRONIC AND PHOTONIC ANALYSIS OF UWMAK-III BLANKET AND SHIELD IN NON CIRCULAR TOROIDAL GEOMETRY

Y. Gohar, C. W. Maynard, E. T. Cheng

FUSION TECHNOLOGY PROGRAM, UNIVERSITY OF WISCONSIN

The nuclear analysis of the UWMAK-III blanket and shield based on the actual shape of the confinement chamber is presented. Neutron and photon transport calculations were carried out by use of two dimensional S_n to account for the toroidal geometry. The effect of the toroidal geometry on the breeding ratio, nuclear heating, atomic displacements and gas production is discussed. The neutron streaming through the slots in the divertor is considered. It is found that the breeding ratio is about 14% greater than the value calculated using a two dimensional X-Y geometry model. The nuclear heating in the relatively unaccessible blanket section nearest the major axis of the torus is about 18% of the total nuclear heating. The wall loading and the gas production in the first wall as one goes around the plasma in the poloidal direction change by factors of order two. The neutron streaming from the divertor zone is far in excess of the toroidal field magnet tolerance. This results in the need for the additional shield in this zone to protect the magnet.

INTRODUCTION

The University of Wisconsin Fusion Design Group has carried out several conceptual reactor design. The first two, UWMAK-I and UWMAK-II,[1,2] were conservative systems based on present day technology. UWMAK-III,[3] described here, is intended to be an advanced plant typical of a mature fusion power economy. High thermal efficiency is desirable and resulted in the choice of a refractory metal for structural purposes. The design criteria beyond this were primarily economic in keeping with the advanced plant concept. Capital costs are to lowest order determined by physical size and this resulted in a considerable effort to reduce the system size for the same power capacity.

The reduction in the size of the reactor chamber increases the 14 MeV neutron wall loading and the refrigeration power required for the superconducting toroidal field magnets. The reactor chamber of UWMAK-III is designed for 1.9 MW/m^2 average neutron wall loading compared to ~1 MW/m^2 in the UWMAK-I and UWMAK-II designs. The increase in the neutron wall loading will cause a short first wall life. To overcome this problem, the first wall must be designed for rapid replacement or protected from radiation damage. Both approaches have been used for UWMAK-III.

In toroidal geometry, the inner blanket and shield closest to the toroidal axis is the most difficult part to maintain because there is little access space. Thus, a special requirement for UWMAK-III is to design the inner blanket and shield for plant life. This places a premium on design simplicity and has resulted in the concept of using a thick graphite wall in front of the inner wall to protect the inner blanket and shield from radiation damage. This ISSEC concept (Internal

Spectral Shifter and Energy Converter) is described in reference[4] in more detail. The ISSEC zone reduces the displacement, helium and hydrogen production rates in the first structural wall and this increases the wall life for the inner blanket. The ISSEC zone is cooled by heat radiation to the first structural wall. The inner blanket is not designed to breed tritium, but only to recover the neutron energy and protect the superconducting toroidal field magnet. This eliminates the tritium removal problem and the potential of attempting to flow liquid lithium in the high magnetic field region.

The desire for high operating temperature dictates the use of refractory metal alloy as the structural material. The molybdenum alloy TZM has been chosen based on good mechanical properties at high temperature as described in reference[3]. From a neutronic point of view, molybdenum is a good choice for shielding, neutron multiplication and energy deposition.

The outer blanket has no ISSEC and uses liquid lithium as the breeding and cooling medium. This results in an adequate breeding ratio and heat generation without help from the inner blanket. The lack of ISSEC causes wall replacement to be comparable to previous designs. However, it eliminates the potential resource problem that would result if beryllium were used as a neutron multiplier and the economic problem of lithium enrichment which would result if adequate performance is required with a full ISSEC.

BLANKET AND SHIELD MODELS FOR NEUTRONIC AND PHOTONIC CALCULATIONS

A schematic representation of the UWMAK-III chamber is shown in Figure 1 where both the plasma and the chamber are noncircular with a low aspect ratio. This configuration was chosen to achieve high power density.[3] The height to width ratio of the plasma is approximately 2, with a 8.1m major radius and a 2.1m half width. The magnetic axis which serves as the plasma axis is not at the geometrical center of the plasma. Since the neutron source distribution is proportional to the square of the ion density, the resulting neutron source will be shifted from the geometrical center of the chamber.

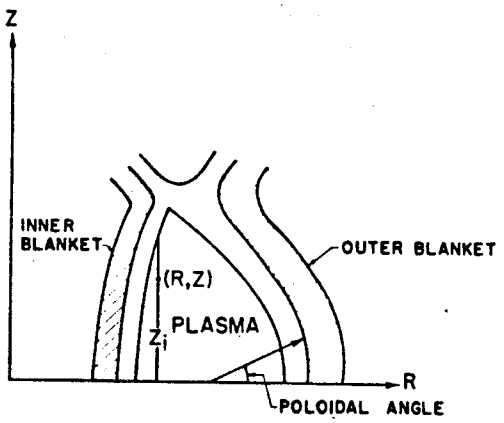

Figure 1. A schematic of UWMAK-III chamber

The neutronic and photonic analysis has been investigated through use of three different models for the reactor geometry. The first model is a one dimensional shell representation. The other two models are two dimensional X-Y and R-Z representations.

The usual one dimensional model used for the neutronic and photonic transport calculations for Tokamak reactors based on an infinite cylinder obtained by considering a vertical cut through the torus. This is expected to be acceptable only when the system has poloidal symmetry, a centered plasma and a high aspect ratio. Actually, the UWMAK-III design employed in the ISSEC concept for the inner blanket, an off center neutron source, and a low aspect ratio, which makes the vertical cut model unacceptable for this design.

The one dimensional model which considers all of the above unique features of UWMAK-III, results from a horizontal cut through the torus at the midplane. This model allows for the inner blanket to be different from the outer one in composition and/or zone thickness. Further, the off-center source can be represented in this model. This takes the low aspect ratio into account properly and for vertically elongated plasma, as in the UWMAK-III design, may represent the midplane results very well. A schematic representation for this model is shown in Figure 2. The choice of zone thicknesses was determined from a one dimensional parametric study. The neutron source distribution has been approximated as

$$S(R) = S_0[1-(\frac{R-900}{180})^2]^3 \quad 1080 \geq R \geq 900,$$

$$S(R) = S_0[1-(\frac{900-R}{360})^2]^3 \quad 540 \leq R \leq 900.$$

Where S_0 is the source value at the magnetic axis (R=900) which is shifted from the geometrical axis.

After the one dimensional analysis has been carried out, it was still of great concern to do the analysis in two dimension to account for the divertor slots, the toroidal effect and the two dimensional source shape. The first two dimensional model is based on a simple representation for the reactor chamber as a rectangular shape in the two dimensional X-Y geometry shown in Figure 3. The neutron source was approximately represented as a function of X and Y, in a vertical plane through the torus as

$$S(X,Y) = S(0,0)[1-(\frac{x-50}{200})^2]^3[1-(\frac{Y}{580})^2]^3$$

$$-150 \leq X \leq 250$$

$$0 \leq Y \leq 580,$$

and

$$S(X,Y) = S(150,Y)[0.01X+2.50]$$

$$-250 \leq X \leq 150$$

$$0 \leq Y \leq 580.$$

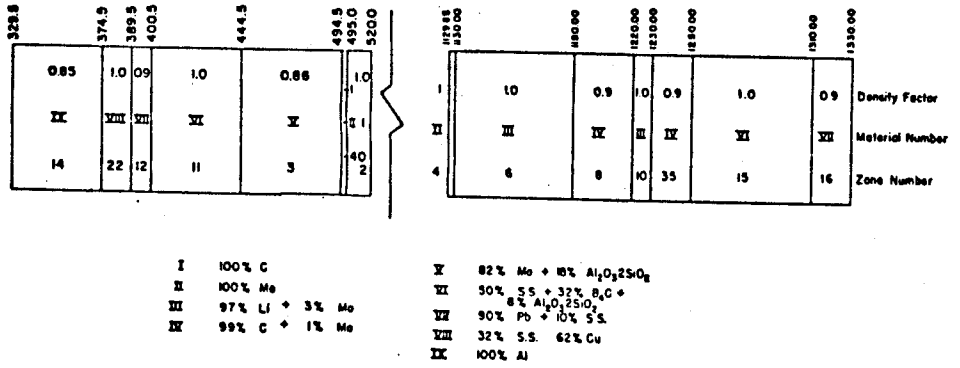

Figure 2. A schematic of UWMAK-III blanket and shield model for one dimensional calculation and R-Z neutronic and photonic calculation at the midplane

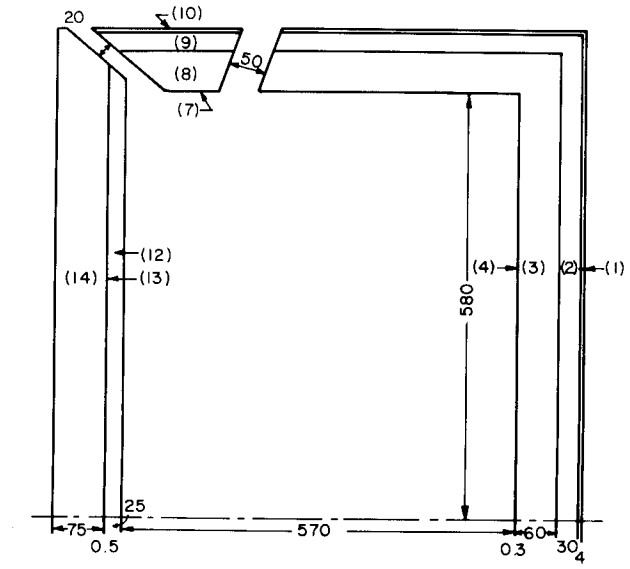

ZONE	COMPOSITION	ZONE	COMPOSITION
1. 3...8. 10	97% Li + 3% Mo	4. 7. 13 -	Mo
2. 9	99% C + 1% Mo	12	C
14	40% B_4C+6% Mo (DENSITY FACTOR .95)		

Figure 3. A schematic of UWMAK-III blanket model used for x-y two-dimensional analysis

This model still does not account for the actual toroidal geometry effect, although it takes care of the other effects mentioned above. At this point, a more realistic model was considered by using two dimensional R-Z geometry to represent the actual shape of the UWMAK-III configurations as shown in Figure 4.

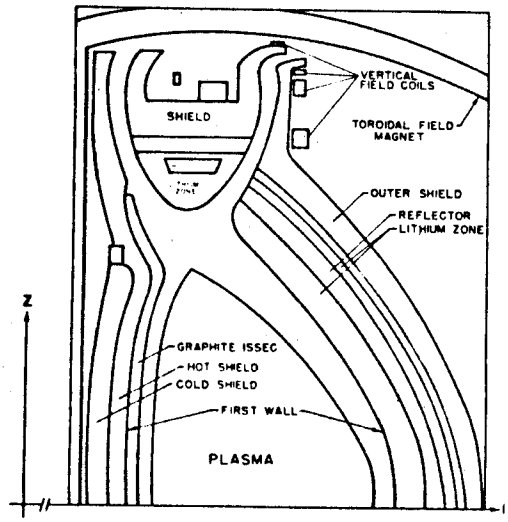

Figure 4. A schematic of UWMAK-III model used for R-Z two-dimensional analysis

The neutron source distribution for the R-Z model has been represented as a function of R and Z as

$$S(R,Z) = S(R,0)[1 - (Z/Z_i)^2]^3$$

$$S(R,0) = S(0,0)[1-((R-900)/180)^2]^3 \qquad 1080 \geq R \geq 900,$$

$$S(R,0) = S(0,0)[1-((900-R)/360)^2]^3 \qquad 540 \geq R \geq 900.$$

Where Z_i is the vertical boundary of the source distribution. The source shift from the geometrical center of the chamber is 90m for the two dimensional R-Z and one dimensional calculation rather than the 50cm shift used in the X-Y calculation. The 90cm shift is based on more recent plasma calculations.[3]

The neutron and gamma cross sections employed in the transport calculation were obtained as acoupled set of 100 neutron and 21 gamma groups generated for EPR calculations[5] by Plaster et al. This data set was generated with AMPX modular code system[6] from the nuclear data in ENDF/B-IV. Due to cost and computer memory limitations, the one hundred neutron group cross sections were collapsed to 46 groups keeping the same fine group structure above 2 MeV as in the original set.

UWMAK-III BLANKET AND SHIELD FEATURES

The inner blanket is helium cooled. This choice is a consequence of several factors. The high wall loading involves increased coolant flow which would result in MHD problems in the high field region if liquid lithium cooling were necessary. As adequate tritium breeding can be achieved in the outer blanket alone, this allow to simplify the design by eliminating tritium recovery in this zone entirely. The helium will pick up little activated wall material and this allows consideration of a direct closed cycle turbine for conversion

of the energy from this zone. The operating temperatures are chosen to achieve good turbine performance and these may be and are quite high with the TZM structure.[3] The inner blanket and shield is essentially shield now and is divided into hot and cooled section with 99.1% of the energy deposited in the hot section. From the neutronic point of view, molybdenum is a good shielding material (high inelastic cross section). The cold shield is designed to minimize the radiation damage and heating to the superconducting magnet. Boron is excluded from the hot shield to prevent production of tritium which in undesirable for the direct cycle helium cooled shield.

The outer blanket was designed to breed adequate tritium for reactor operation and to recover the neutron energy. The liquid lithium is the most suitable coolant and breeding material for this zone of the reactor.

NEUTRONIC AND PHOTONIC ANALYSIS

Based on the above discussion and parametric survey, to maximize the tritium production rate, Figure 5 shows the equi-breeding contours as a function of the percent structure and ^{6}Li in the breeding zones for UWMAK-III blanket (the outer breeding zone behind the reflector zone is 4cm in this particular survey) using the multipoint interpolation method.[7] The UWMAK-III blanket and shield are specified as shown in Figures 2 and 4. On the left is the inner-most shield starting at a major radius of 389.5cm, the inner structural wall is at 495cm and the ISSEC ends at 520cm. The plasma is centered at 810cm, but the source peaks at 900cm in the one dimensional and R-Z two dimensional calculations based on a better plasma calculation that was available for the earlier 50cm shift used for X-Y two dimensional calculations. The outer blanket and shield occupy the region between 1130 and 1330 cm. The outer structural wall is 0.3cm thick which is adequate for the stress in the low pressure liquid lithium system. The inner blanket is helium cooled. The high pressure required for the coolant results in the need for a 0.5cm TZM wall as the first structure wall of the inner blanket. The liquid lithium zones are 60cm and 10cm with 3% TZM by volume. The graphite reflector zones are 30 and 10cm with 1% TZM structure by volume. The ISSEC thickness is 25cm carbon in front of the first structural wall of the inner blanket.

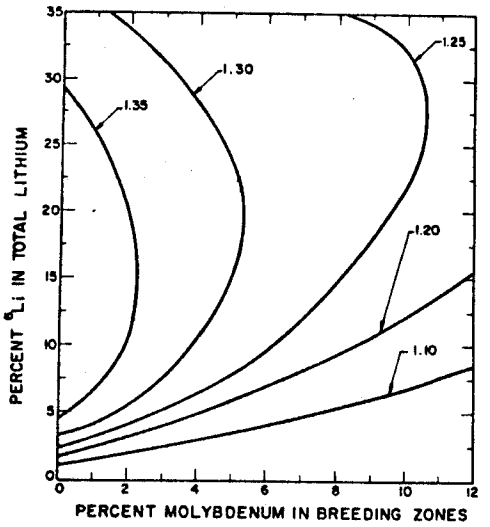

Figure 5. Equi-Breeding Ratio Contours

Summary results for S_6-P_3 one dimensional calculation using ANISN program[8] are given in Table 1 and Table 2 for tritium production and the nuclear heating per zone. The breeding ratio of 1.37 is quite satisfactory. However, this is expected to be higher than the actual value, since the model does not account for curvature of the media in the poloidal direction and the source distribution in the axial direction.

TABLE 1. Tritium Production Rates Per Fusion Neutron From One-Dimensional Calculations

Zone	$^{6}Li(n,\alpha)T$	$^{7}Li(n,n'\alpha)T$	Total
6	0.7603	0.5485	1.3088
10	0.0587	0.0018	0.0606
Total	0.8190	0.5503	1.3693

TABLE 2. Neutron and Gamma Heating by Zone Per Fusion Neutron From One-Dimensional Calculations (MeV/DTN)

Zone	Neutron Heating	Gamma Heating	Total/Zone
22	2.441-7a	2.2271-6	2.471-6
12	7.150-8	2.555-6	2.626-6
11	4.013-3	2.777-3	6.790-3
3	3.777-2	7.207-1	7.585-1
40	1.292-2	4.329-1	4.458-1
1	1.625	6.413-1	2.266
4	8.836-2	6.588-1	7.472-1
6	1.006+1	1.362	1.142+1
8	3.459-1	5.568-1	9.027-1
10	3.068-1	4.684-2	3.537-1
35	2.598-2	9.391-2	1.199-1
15	3.675-2	5.908-2	9.583-2
16	4.752-7	1.045-5	1.092-5
Total	12.54	4.575	17.12

a2.441-7 = 2.441×10^{-7}

The total energy deposition per D-T neutron in the blanket and shield is 17.12 MeV. This is 0.56 MeV greater than the corresponding figure for UWMAK-I design. This increased energy production is primarily related to molybdenum performance in the outer blanket. The (n,2n) reaction in the molybdenum contributes about 0.1 neutrons per 14 MeV neutron in the outer blanket which goes mainly to react with the lithium. Also the choice of carbon for reflector zone and the less percent structure used for the outer blanket had little effect in increasing the breeding ratio and energy deposited per D-T neutron. In comparison with UWMAK-II, the results show the energy per fusion neutron is less by 0.94 MeV even though UWMAK-II has an even lower breeding ratio as noted in Table 3. The reason for the higher UWMAK-II energy production is that the bredding is mainly from ^{6}Li reactions (90% enriched lithium) which are highly exothermic reactions. Neutron multiplication comes from the (n,2n) reaction in beryllium which has a low Q value. The energy leakage from UWMAK-III to the superconducting magnet is less than the corresponding value in UWMAK-I as shown in Table 3.

TABLE 3. Tritium Breeding, Nuclear Heating and Energy Leakage in the UWMAK-III Design in Comparison with UWMAK-I and II Based on One-Dimensional Calculations

Parameter	III	II	I
$^{6}Li(n,\alpha)t$	0.8190	1.1801	0.8835
$^{7}Li(n,n'\alpha)T$	0.5503	0.0034	0.6037
Tritium Breeding Ratio	1.3693	1.1835	1.4872
Neutron Heating[a]	12.71	13.11	12.43
Gamma Heating[a]	4.62	4.95	4.13
Total Heating[a]	17.12	18.06	16.56
Energy Leakage to the Magnet[a]	1.47×10^{-6}	1.02×10^{-6}	1.53×10^{-5}

a In Units of MeV/DTN.

TWO DIMENSIONAL CALCULATIONS

An X-Y two dimensional calculation which accounted for the poloidal change in the source and geometry are carried out. A summary of the results is shown in Tables 4 and 5. This calculation was accomplished for the blanket using the two dimensional S_n program DOT[9] in the S_4P_3 approximation. The tritium production rate is 1.076 per

D-T neutron. Although this result is considerably less than the results from the one dimensional model, it is still adequate and accounts for the lack of inner blanket breeding and for leakage. In fact, this result is expected to be a lower bound since the toroidal effect should increase the total outer blanket contribution. The total neutron heating is about 11.85 MeV per D-T neutron compared with 12.54 MeV from the one dimensional calculation. This is in the direction expected for the lower breeding ratio.

TABLE 4. Tritium Production Rates by Zone Per Fusion Neutron From Two-Dimensional X-Y Calculation

Zone	$^{6}Li(n,\alpha)T$	$^{7}Li(n,n'\alpha)T$	Total/Zone
1	0.0253	0.0007	0.0260
3	0.5340	0.3684	0.9024
8	0.0771	0.0602	0.1373
10	0.0074	0.0009	0.0083
Total	0.6438	0.4302	1.0740

TABLE 5. Neutron and Gamma Heating by Zone Per Fusion Neutron From Two-Dimensional X-Y Calculations (MeV/DTN)

Zone	Neutron Heating	Gamma Heating	Total/Zone
1	0.1300	0.0139	0.1439
2	0.2630	0.3467	0.6097
3	6.9701	0.5960	7.5641
4	0.0195	0.0759	0.09564
7	0.0014	0.0059	0.0073
8	1.0795	0.0819	1.1615
9	0.2083	0.0955	0.3038
10	0.0460	0.0046	0.0506
12	2.4505	0.660	3.1105
13	0.0038	0.209	0.2128
14	0.6744	4.233	4.9074
Total	11.8466	6.3204	18.1670

The two dimensional R-Z calculations have now been carried out to account for the actual geometry including all the factors discussed before for a complete evaluation of the UWMAK-III performance. The two dimensional S_n program DOT[9] was used in the S_6-P_3 approximation in R-Z geometry to carry out the calculation. The geometry model used is shown in Figure 4. The integral results are shown in Tables 6 and 7.

TABLE 6. Tritium Production Rates by Zone Per Fusion Neutron From R-Z Toroidal Calculation

Zone	$^{6}Li(n,\alpha)T$	$^{7}Li(n,n'\alpha)T$	Total/Zone
6	0.6675	0.4021	1.0696
10	0.0770	0.0334	0.1104
7	0.0683	0.0032	0.0715
Total	0.8128	0.4387	1.2515

Table 6 lists the tritium production rates per D-T neutron in each zone. The total breeding ratio is 1.25. The breeding ratio from the R-Z calculation is thus greater than from the X-Y calculation by about 16%. In fact, this increase in the breeding ratio is not completely due to the correction from the toroidal effect. Comparison with tritium production rates per zone from Table 4 shows that the toroidal effect increases the breeding by about 9%. The remaining 7% increase is due to a change in the thickness of the last zone of the outer blanket and better neutron reflection from the shielding material. The last zone of the outer blanket (Zone 10, Figure 2) has been increased in thickness from 4 to 10cm, as required by mechanical consideration for the lithium headers.

On the other hand, the one dimensional calculation shows a higher value for the breeding ratio by about 22% for the main breeding zone and 5% on the average as can be seen from Tables 1 and 6.

Summary results of the heat deposition per zone are given in Tables 7 and 8. The R-Z calculational result is 17.57 MeV per D-T neutron deposited in the blanket and shield. It can be noted from Table 8 that the heat deposition in the outer blanket is a factor of 4 times the heat deposition in the inner blanket (including the ISSEC). This distribution for the heat deposition is approximately the same as obtained from the one dimensional study and differs from the X-Y calculation which shows only a factor of two for this ratio.

TABLE 7. Neutron and Gamma Heating Rates Per Fusion Neutron by Zone From R-Z Toroidal Calculation (MeV/DTN)

Zone	Neutron Heating	Gamma Heating	Total Heating/Zone
2	1.3481	0.6775	2.0256
3+40	0.0698	1.5886	1.6583
4	0.0841	1.0409	1.1250
5	0.0117	0.1781	1.1898
6	8.0960	1.7348	9.9308
10	0.3711	0.0809	0.4520
7	0.7874	0.1815	0.9689
8	0.3136	0.4979	0.8115
36+9	0.0466	0.0808	0.1274
Shielding			0.3803
Total			17.5696

The heat deposition in the first wall of the outer blanket behind the ISSEC is given in Figure 6 as a function of the poloidal angle. The heat deposition shows a behavior similar to the first group neutron flux, but the maximum to minimum value for the outer wall is about 1.4 compared to the corresponding ratio for the first group neutron flux which is about 2. In fact, the first wall heating is due to gamma heating from inelastic scattering which explains the similarity to the high energy neutron flux distribution.

TABLE 8. Power Distribution For UWMAK-III

Zone	Power Percent
ISSEC	9.6
inner blanket (Hot shield)	7.9
outer blanket	57.9
Divertor	6.1
Divertor plates (α particles)	16.7
inner shield	0.9
outer shield	0.6
divertor shield	0.3

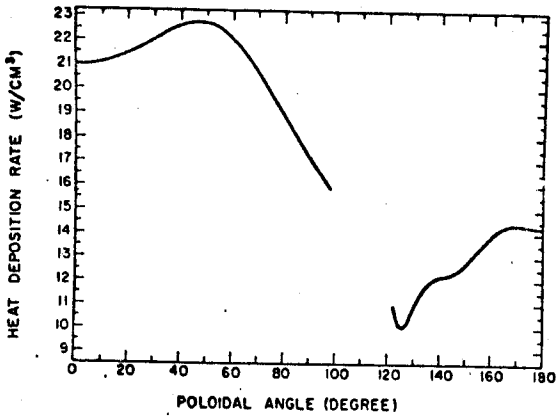

Figure 6. Heat deposition rate in the first wall

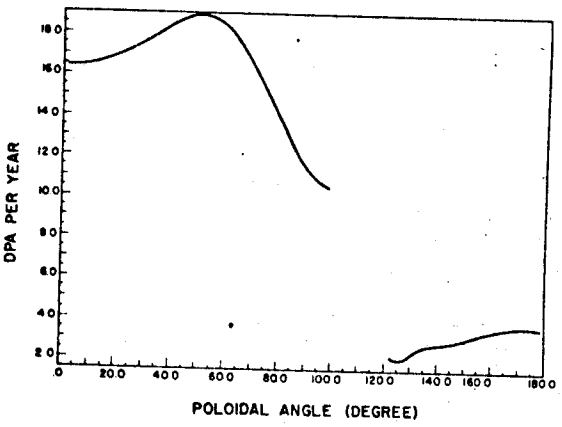

Figure 7. Displacement rate in the first wall

The displacement rates are 3.7 and 16.4 dpa/year in the inner and outer wall at the midplane respectively as shown in Figure 7. This shows that the effect of the ISSEC is to reduce the dpa rate by a factor of 4 to 5 and also reduce the helium and hydrogen production rates by factors of 8 and 12 respectively, as shown in Figures 8 and 9.

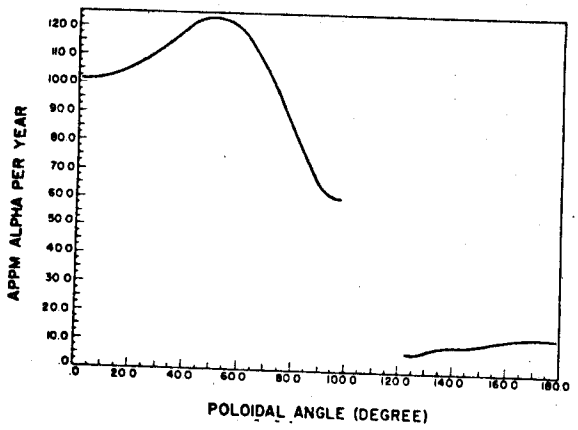

Figure 8. Alpha generation rate in the first wall

The heat deposition rate in the graphite ISSEC is plotted in Figure 10 as a function of the poloidal angle at a depth of 4 cm. It shows a maximum of 9.6 w/cm^3 at the midplane and drops to about 5 w/cm^3 at the end. Most of the heat deposition in the ISSEC is due to neutron heating, particularly the high energy neutron flux. This explains the similarity between the heating curve and the high energy flux. The displacement and helium production rates in the ISSEC show similar behavior to the nuclear heating which is expected.

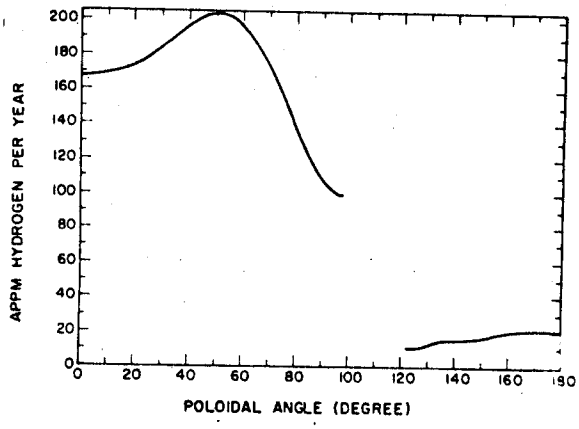

Figure 9. Hydrogen generation rate in the first wall

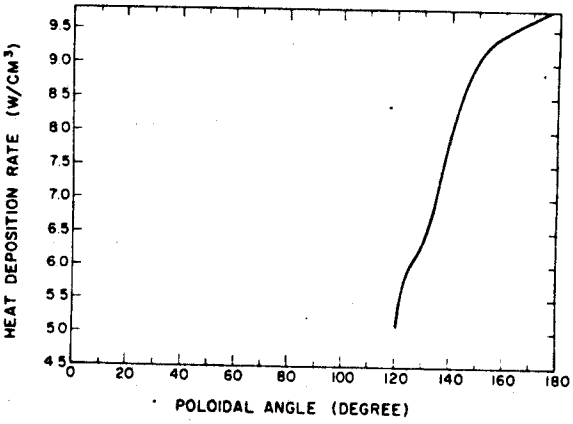

Figure 10. Heat deposition rate in the graphite ISSEC

The tritium production rates and heat deposition at three different depths in the outer blanket and in the lithium zone behind the reflector are shown in Figures 11 and 12. It is clear that the heat deposition and tritium production rates at a depth of 5cm in the outer blanket behaves in a manner quite similar to the high energy neutron

flux. At the second depth in the lithium zone (25cm), most of the contribution for the heat deposition and the tritium production still comes from the high energy neutron flux particularly at the midplane. However, at a poloidal angle of about 60^{o}, the low energy group contributes strongly to the heating rates through the highly exothermic reaction with ^{6}Li which shows a peak in the

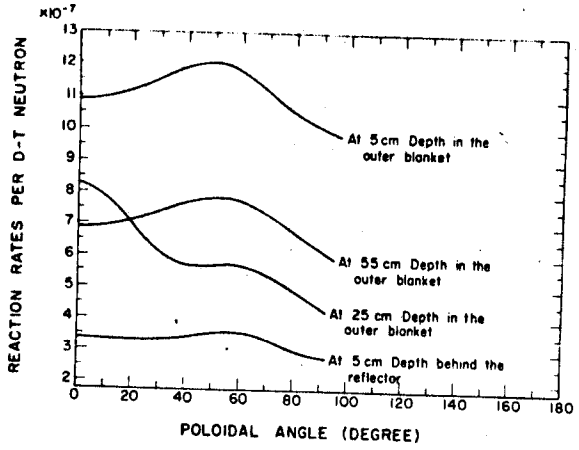

Figure 11. Tritium production rates

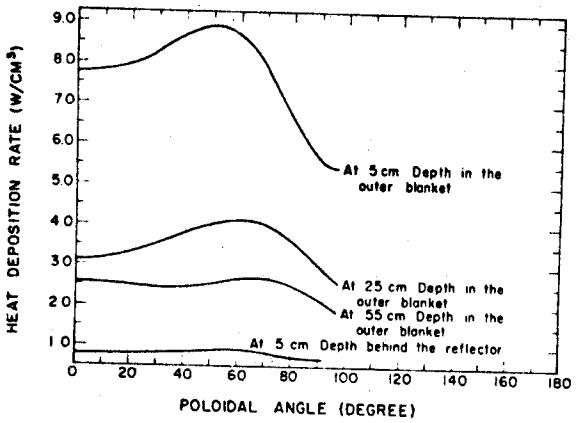

Figure 12. Heat deposition rate in the outer blanket

heating rates at this angle, but little pump in the tritium production rates at the same depth. At the end of the lithium zone and behind the reflector, the contribution is mainly from the low energy neutron flux which is almost uniform in the poloidal direction.

Figure 13 shows the energy deposited in the toroidal field magnet as a function of the poloidal angle. It is clear that the nuclear heating increases dramatically near the divertor slots. The helium production rate in the poloidal direction is shown in figure 14.

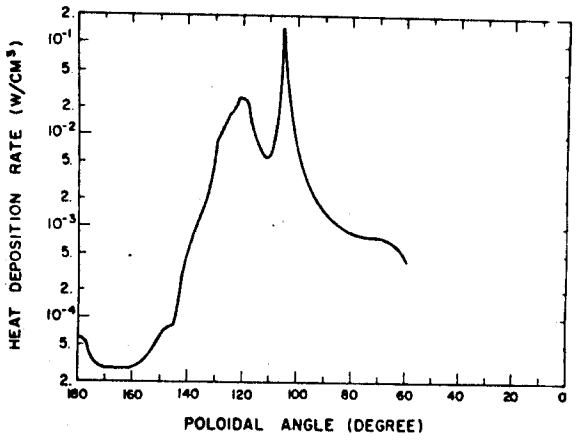

Figure 13. Heat deposition rate in the toroidal field magnet

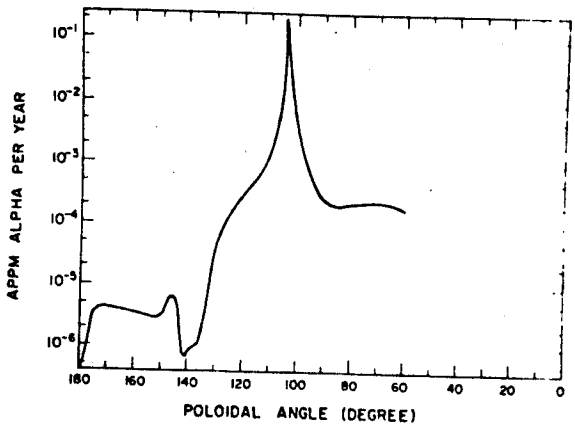

Figure 14. Alpha generation rate in the toroidal field magnet

The heat deposition and the helium production rates can be understood clearly by investigating Figure 15 which shows the neutron flux distribution over all of the reactor. The streaming through the divertor slots is readily observed. The heat deposition curve shows two peaks corresponding to the divertor slots, where both the low and high neutron energy contribute to the heat deposition. The helium production rate shows a single peak since the streaming in the left slot of the divertor is due to low energy neutrons which do not contribute to the helium production rate. Based on these results, additional shields of 20cm thickness has been added in front of the slots to protect the toroidal field magnet.

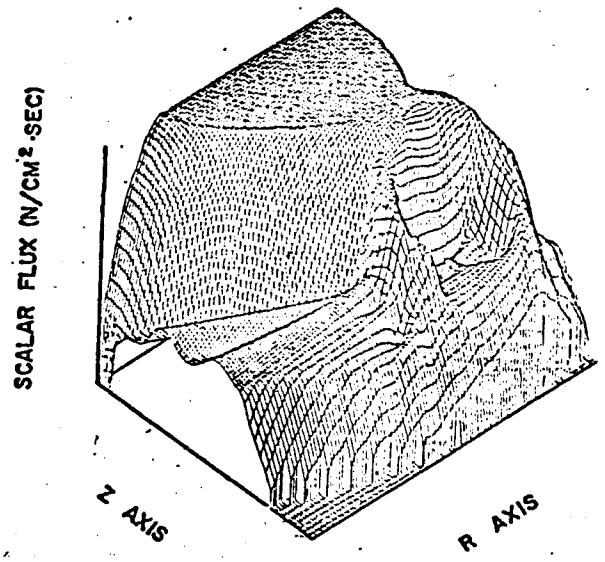

Figure 15. The first energy neutron flux distribution over the entire reactor

CONCLUSIONS

The nuclear analysis of a low aspect ratio Tokamak reactor using the actual two dimensional (R-Z) geometric representation reveals some important changes in the results. It is found that:

(a) The breeding ratio is about 16% greater than the value calculated using a two dimensional (X-Y) geometry model, [10] and about 9% less than the value calculated using a one dimensional (R) model.

(b) The nuclear heating and the gas production in the first wall changes by a factor of the order of two in the poloidal direction.

(c) The neutron streaming through the divertor slots has a major effect on the shield design for the toroidal field magnets.

(d) The total nuclear heating is about the same from the different calculational models within ± 1 Mev/fusion neutron.

These results illustrate the importance of the actual geometry for the analysis of a low aspect ratio blanket and shield.

REFERENCES

1. B. Badger, et al., "A Wisconsin Toroidal Fusion Reactor Design - UWMAK-I," UWFDM-68, Univ. of Wis. (1974).

2. B. Badger, et al., "A Conceptual Tokamak Reactor Design - UWMAK-II," UWFDM-112, Univ. of Wis. (1975).

3. B. Badger, et al., "A Noncircular Tokamak Power Reactor Design - UWMAK-III," UWFDM-150, Univ. of Wis. (1976).

4. R. W. Conn, et al., "New Concepts for Controlled Fusion Reactor Blanket Design," UWFDM-115, Univ. of Wis. (1974).

5. D. M. Plaster, R. T. Santoro, W. E. Ford III, "Coupled 100 Group Neutron and 21 Group Cross Section for EPR Calculations," ORNL-TM-4872, Oak Ridge National Lab. (1975).

6. N. M. Greene, et al., "AMPX: A Modular Code System for Generating Coupled Multigroup Neutron-Gamma Libraries from ENDF/B," ORNL-TM-3706, Oak Ridge National Laboratory (1976).

7. E. T. Cheng and R. W. Conn, "A Multipoint Interpolation Method Based on Variational Principles for Functionals of the Solution to Linear Equations," Journal of Mathematical Physics, Vol. 17, No. 5, May 1976.

8. W. W. Engle, Jr., "A User Manual for ANISN, A One-Dimensional Discrete Ordinates Transport Code with Anisotropic Scattering," Report H-1693, Computing Technology Center, Union Carbide Corporation (1967).

9. W. A. Rhoades and F. R. Mynatt, "The DOT-III Two-Deinesional Transport Code," ORNL-TM-4280, Oak Ridge National Laboratory (1975).

10. C. W. Maynard, R. W. Conn, Y. Gohar, Trans. Am. Nucl. Soc. 22, 16 (1975).